Vol 13 No 9, September 2004
1009-1963/2004/13(09)/1553-07

Chinese Physics

© 2004 Chin. Phys. Soc.
and IOP Publishing Ltd

Vortex domain structures and dc current dependence of magneto-resistances in magnetic tunnel junctions*

Wei Hong-Xiang(魏红祥)[a)b)], Lu Qing-Feng(路庆凤)[a)], Zhao Su-Fen(赵素芬)[b)], Zhang Xie-Qun(张谢群)[b)], Feng Jia-Feng(丰家峰)[b)], and Han Xiu-Feng(韩秀峰)[b)†]

[a)] *Department of Physics and Communication, Henan Normal University, Xinxiang* 453002, *China*
[b)] *State Key Laboratory of Magnetism, Institute of Physics, Chinese Academy of Sciences, Beijing* 100080, *China*

(Received 13 April 2004; revised manuscript received 18 June 2004)

Microfabrication and the magneto-transport characteristics of the magnetic tunnel junctions (MTJs) with a spin-valve-type structure of Ta (5nm)/$Ni_{79}Fe_{21}$ (25nm)/$Ir_{22}Mn_{78}$ (12nm)/$Co_{75}Fe_{25}$ (4nm)/Al(0.8nm) oxide/$Co_{75}Fe_{25}$ (4nm)/$Ni_{79}Fe_{21}$ (20nm)/Ta(5nm) were investigated in this paper. A series of experimental data measured with a MTJ was used to verify a magnon-assisted tunnelling model and theory. Furthermore, a micromagnetics simulation shows that the butterfly-like vortex domain structures can be formed under a current-induced Oersted field, which decreases the net magnetization values of the ferromagnetic electrodes under a large dc current (i.e., in high voltage regimes). It is one of the main reasons for the tunnel magnetoresistance ratios to decrease significantly at high voltage biasing.

Keywords: magnetic tunnel junction, tunnel magnetorisistance, spin-electron transport, magnon-assisted tunnelling, vortex domain structure

PACC: 7475, 7430C, 7360T, 7560N

1. Introduction

Research in magnetic tunnel junctions (MTJs) and tunnel magnetorisistance (TMR) effect, no matter whether the aim of which is materials development or device fabrication, has attracted the attention of researchers in both academic and industrial sectors due to the promising applications of MTJs in magnetoresistive random access memory (MRAM), magnetic read head and other high-sensitivity field sensors.[1−7] In recent years, although a series of advancement in both experimental and theoretical researches in MTJ materials and the TMR effect has been achieved,[8−16] some magnetoelectronic properties have not yet been fully evaluated using the present spin-electron transport theories developed for MTJs. For example, the difference between experimental data and theoretical evaluations of the dc bias voltage dependence of the TMR effect is also an area of dispute.[8,11] Therefore, further investigations on these unclear topics are necessary in order to improve the understanding of the MTJ structure, thereby to facilitate the development and enhancement of MTJ-based devices.

In this paper, we present the fabrication and the magneto-transport characteristics of the MTJs with a spin-valve-type layered structure of Ta (5nm) / $Ni_{79}Fe_{21}$ (25nm) / $Ir_{22}Mn_{78}$ (10nm) / $Co_{75}Fe_{25}$ (4nm) / Al(0.8nm)-oxide/$Co_{75}Fe_{25}$ (4nm) / $Ni_{79}Fe_{21}$ (25nm) / Ta(5nm). A series of experimental data obtained for a MTJ is used to verify the magnon-assisted tunnelling model and theory. Our micromagnetics simulation shows that the butterfly-like vortex domain structures can decrease the net magnetization of the ferromagnetic(FM) electrodes under high voltage biasing, which can result in a significant decrease of TMR ratios

$$\mathrm{TMR}(V,T) = \frac{R^{\mathrm{AP}}(V,T) - R^{\mathrm{P}}(V,T)}{R^{\mathrm{P}}(V,T)} \qquad (1)$$

in high bias voltage (i.e., large dc current) regimes.

*Project supported by the "Hundred Talents Project" of Chinese Academy of Sciences and in part by the State Key Program of Basic Research of China (Grant No 2001CB610601) the National Natural Science Foundation of China (Grant No 10274103).
†Corresponding author: E-mail: xfhan@aphy.iphy.ac.cn

2. Experimental method

The MTJ films were first deposited on the substrate of Si/SiO_2 using an ULVAC TMR R&D magnetron sputtering system (MPS-4000-HC7) with ultrahigh vacuum and three chambers. All the deposition processes were carried out at a base pressure of about 3×10^{-6} Pa without breaking the vacuum in any process. The Al–O insulating layer was formed by inductively coupled plasma oxidation with an oxidation time of 40s in a mixture of oxygen and argon at a pressure of 1.0Pa. Tunnel junctions with small active areas ranging from 10×10 to 5×5 μm^2 were fabricated using a micro-fabrication technique. The optical lithography combined with Ar ion-beam etching was used to pattern the junction area. The annealing temperature and time for these MTJs obtained were inferred to be around 275°C for 1h. TMR curves at a dc bias voltage of 1mV, the TMR ratio and junction resistance R versus dc bias voltage curves at room temperature for the tunnel junction were measured using the dc four-probe method in a magnetic field up to 1000Oe (1Oe=79.5798A/m). The TMR curves between 4.2 and 300K were measured with a physical properties measurement system (PPMS).

In order to keep the same values of the intrinsic parameters for calculating the magnetoelectric properties of a MTJ self-consistently, it is necessary to use the same MTJ for all the experimental measurements. Therefore, a series of experimental data obtained for a spin-valve-type MTJ with a size of $8\times8\mu m^2$ was used to verify the magnon-assisted tunnelling theory and calculations.

3. Method of calculation

Recently, a spin-electron polarization tunnelling model developed by Zhang *et al*[8] based on thermal or bias-voltage-assisted magnon excitations by the tunnelling electrons during the tunnel process has been extended by defining an anisotropic-wavelength-cutoff energy E_c^γ of spin-wave spectrum in MTJs.[11] In this extended magnon-assisted tunnelling theory, the conductance $G=\dfrac{I}{V}$ at 0 K and zero voltage is denoted as $G^\gamma(0,0)$, where γ=P or AP represents the parallel (P) or antiparallel (AP) alignment of the magnetization of the two FM electrodes. The added components for the bias voltage and temperature dependences are indicated by $\Delta G^\gamma(V,T)$. Then, more concise explicit function expression for the bias voltage or/and temperature dependences of normalized conductance, resistances, and TMR ratio at 0K, zero bias, or finite bias and temperature can be written respectively as the following with a unique set of intrinsic parameters:

$$\frac{G^\gamma(V,T)}{G^\gamma(0,0)}=1+QC^\gamma\nu(V)+QC^\gamma\frac{2Sk_BT}{E_m}\tau(T), \quad (2)$$

where

$$Q=\frac{1}{|T^d|^2/|T^J|^2+2S^2}, \quad (3)$$

$$C^\gamma=\begin{cases}\xi, & \text{when} \quad \gamma=\text{P},\\ 1/\xi, & \text{when} \quad \gamma=\text{AP},\end{cases} \quad (4)$$

$$\xi=\frac{2\rho_M\rho_m}{\rho_M^2+\rho_m^2}=\frac{2}{\rho_M/\rho_m+\rho_m/\rho_M}, \quad (5)$$

$$\nu(V)=\begin{cases}SeV/E_m, & \text{for} \quad eV<E_m,\\ S(2-E_m/(eV)), & \text{for} \quad eV>E_m,\end{cases} \quad (6)$$

$$\begin{aligned}\tau(T)&=-\ln[1-e^{-E_c^\gamma/k_BT}]\\ &=\ln\left(\frac{k_BT}{E_c^\gamma}\right), \quad \text{for} \quad k_BT>E_c^\gamma.\end{aligned} \quad (7)$$

The definitions of the parameters and subfunctions mentioned above have been reported earlier.[6,11] The parameters of T^d and T^J represent the direct and spin-dependent transfer matrix element, respectively. Therefore, the bias voltage and temperature dependence of the resistance $R^\gamma(V,T)$ can be easily deduced from Eq.(1) by the reciprocal transformation between the conductance and resistance:

$$\frac{R^\gamma(V,T)}{R^\gamma(0,0)}=\frac{1}{1+QSC^\gamma[eV/E_m+(2k_BT/E_m)\ln(k_BT/E_c^\gamma)]}, \quad \text{for} \quad eV<E_m \quad \text{and} \quad k_BT>E_c^\gamma, \quad (8)$$

$$\frac{R^\gamma(V,T)}{R^\gamma(0,0)}=\frac{1}{1+QSC^\gamma[(2-E_m/(eV))+(2k_BT/E_m)\ln(k_BT/E_c^\gamma)]}, \quad \text{for} \quad eV>E_m \quad \text{and} \quad k_BT>E_c^\gamma, \quad (9)$$

$$\frac{R^{AP}(0,0)}{R^P(0,0)}=\frac{\rho_M^2+\rho_m^2}{2\rho_M\rho_m}=\frac{1}{\xi}. \quad (10)$$

When $eV\ll E_m$ and $k_BT>E_c^\gamma$, the bias voltage and temperature dependence of TMR ratio can be deduced as follows:

$$\begin{aligned}\mathrm{TMR}(V,T) =& \frac{R^{\mathrm{AP}}(V,T) - R^{\mathrm{P}}(V,T)}{R^{\mathrm{P}}(V,T)} \\ =& \left(\frac{1}{\xi}\right)\left[\frac{1+QS\xi[eV/E_{\mathrm{m}} + (2k_{\mathrm{B}}T/E_{\mathrm{m}})\ln(k_{\mathrm{B}}T/E_{\mathrm{c}}^{\mathrm{P}})]}{1+(QS/\xi)[eV/E_{\mathrm{m}} + (2k_{\mathrm{B}}T/E_{\mathrm{m}})\ln(k_{\mathrm{B}}T/E_{\mathrm{c}}^{\mathrm{AP}})]}\right] - 1 \\ =& [1/\xi - 1] - QS\left\{\left(\frac{1}{\xi^2} - 1\right)\frac{eV}{E_{\mathrm{m}}} + \frac{2k_{\mathrm{B}}T}{E_{\mathrm{m}}}\left[\frac{1}{\xi^2}\ln\left(\frac{k_{\mathrm{B}}T}{E_{\mathrm{c}}^{\mathrm{AP}}}\right) - \ln\left(\frac{k_{\mathrm{B}}T}{E_{\mathrm{c}}^{\mathrm{P}}}\right)\right]\right\}, \qquad (11)\end{aligned}$$

$$\mathrm{TMR}(0,0) = \frac{R^{\mathrm{AP}}(0,0) - R^{\mathrm{P}}(0,0)}{R^{\mathrm{P}}(0,0)} = 1/\xi - 1 = 2P^2/(1-P^2). \qquad (12)$$

In Eq.(12), TMR(0, 0) is the TMR ratio of the MTJs at 0 K and zero bias, which is corresponding to the Julliere's formula at 0 K and zero bias.[17] It can be seen from Eqs.(4) and (12) that the TMR(0,0) can be determined only by the density of states of the itinerant electrons (i.e. spin-polarization P) of the two FM electrodes.

When $eV > E_{\mathrm{m}}$ and $k_{\mathrm{B}}T > E_{\mathrm{c}}^{\gamma}$, a similar explicit function expression for the bias voltage and temperature dependence of TMR ratio also can be deduced using Eq.(8):

$$\begin{aligned}\mathrm{TMR}(V,T) =& \frac{R^{\mathrm{AP}}(V,T) - R^{\mathrm{P}}(V,T)}{R^{\mathrm{P}}(V,T)} \\ =& \left(\frac{1}{\xi}\right)\left[\frac{1+QS\xi[(2 - E_{\mathrm{m}}/(eV)) + (2k_{\mathrm{B}}T/E_{\mathrm{m}})\ln(k_{\mathrm{B}}T/E_{\mathrm{c}}^{\mathrm{P}})]}{1+(QS/\xi)[(2 - E_{\mathrm{m}}/(eV)) + (2k_{\mathrm{B}}T/E_{\mathrm{m}})\ln(k_{\mathrm{B}}T/E_{\mathrm{c}}^{\mathrm{AP}})]}\right] - 1. \qquad (13)\end{aligned}$$

Therefore, the main intrinsic magnetoelectric properties of a MTJ can be evaluated by using these formulations with a unique set of intrinsic parameters. The first parameter is the Curie temperature T_{C} of the ferromagnetic electrode, which can determine the maximum energy of the magnon excitation by $E_{\mathrm{M}} = 3k_{\mathrm{B}}T_{\mathrm{C}}/(2S+1)$. The second parameter is the parameter ξ, which is related with the ratio of density of state for majority (ρ_{M}) and minority (ρ_{m}) itinerant electrons of the FM electrodes at the interfaces between FM/I/FM layers, which can determine the value of effective spin-polarization of the two FM electrodes. These two parameters are the intrinsic properties of the FM electrode material. Other parameters are the spin-dependent matrix-element ratio (i.e. $|T^{\mathrm{d}}|^2/|T^{\mathrm{J}}|^2$), which can be determined by resolving the barrier Hamiltonian[8] and the anisotropic-wavelength-cutoff energies $E_{\mathrm{c}}^{\mathrm{AP}}$ and $E_{\mathrm{c}}^{\mathrm{P}}$ of the spin-wave spectrum for MTJ. They are the structural parameters of the MTJ.

In principle, these intrinsic parameters in formulations, i.e. $E_{\mathrm{m}}(T_{\mathrm{C}}, S)$, $\xi(\rho_{\mathrm{M}}/\rho_{\mathrm{m}})$, $Q(|T^{\mathrm{d}}|^2/|T^{\mathrm{J}}|^2)$, $E_{\mathrm{c}}^{\mathrm{AP}}$ and $E_{\mathrm{c}}^{\mathrm{P}}$, can be pre-determined by experimental measurements or using the first-principle calculation at 0 K and zero bias voltage for a MTJ with the three key layers of FM/I/FM. However, in this paper we assume that they are adjustable parameters, and then find each one of them uniquely by fitting the bias or/and temperature dependence of resistances (conductances) and TMR ratio.

4. Results and discussion

Figure 1 shows the TMR curves measured at 4.2K (a) and room temperature (b) for a MTJ after annealing at 275°C for 1h. The area of the junction S is 8×8 μm^2. The experimental data of TMR was measured by the PPMS with a dc bias of 1 mV. A high TMR ratio of 59.8% is observed at 4.2K, which is much higher than the 42.3% of room temperature TMR ratio mainly due to the decrease of magnon excitations as well as the absence of phonon excitations.

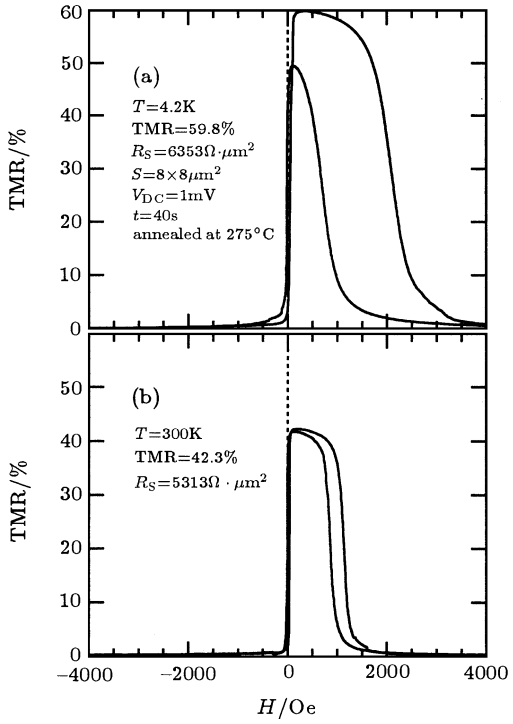


Fig.1. TMR curve at 4.2K (a) and 300K (b) for a representative annealed MTJ, measured at room temperature under a dc bias voltage of 1mV.(1Oe=79.5798A/m).

The experimental data presented in Figs.2–5 were all measured using the same MTJ after annealing as that used in Fig.1. Figure 2 shows the tunnel current I (a) and dynamic conductance $\mathrm{d}I/\mathrm{d}V$ (b) as functions of the dc bias voltage at 4.2K for AP and P magnetic configurations. The increase of the current in AP alignment of magnetization of the two electrodes is slower than that in P alignment, as shown in Fig.2(a), due to the resistance of the AP configuration being larger than that of the P configuration. The effective barrier heights ϕ_1 and ϕ_2 and the barrier width d were obtained by fitting the current I versus dc bias voltage V curves to Simmons' equation, with an asymmetric potential barrier in the insulating layer between the top and bottom magnetic electrodes.[18,19] The effective barrier heights ϕ_1 and ϕ_2, barrier width d, and resistance-area product R_S of the annealed MTJ are 2.62 and 2.73 eV, 0.76 nm, and 6365 $\Omega \cdot \mu\mathrm{m}^2$, respectively, at room temperature. The effective barrier width d is close to the deposited Al thickness of 0.80 nm. The increase of conductance with increasing dc bias voltage is faster for AP alignment as shown in Fig.2(b). It is because the increase of the conductance is proportional to $1/\xi$ for AP and to ξ for P alignment while $1/\xi$ is always larger than ξ, as shown in Eqs.(1), (3), and (4).

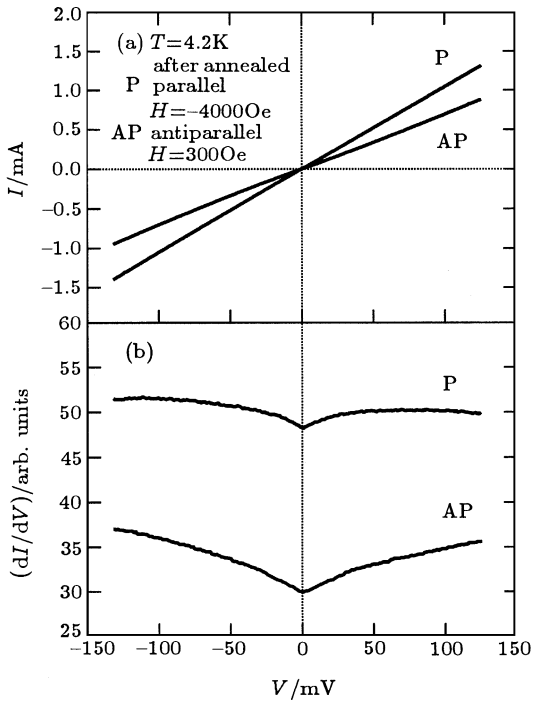


Fig.2. Tunnel current (a) and conductance (b) as functions of dc bias voltage measured at room temperature for the same annealed MTJ as that used in Fig.1.

Figure 3 shows the dc bias voltage dependence of $\mathrm{TMR}^{\mathrm{IV}}$ ratio at T=4.2K, while V varies from 0 to ±120mV for the junction. $\mathrm{TMR}^{\mathrm{IV}}$ is deduced from the $I-V$ curves in Fig.2. Solid squares are the experimental data and the solid lines represent the calculated values using Eq.(10) with E_{m}=121mV and $T \simeq$0K. In such a case, one value of Q=0.0567, i.e. the spin-dependent matrix-element ratio of $|T^{\mathrm{d}}|^2/|T^{\mathrm{J}}|^2$=13.1, can be first uniquely obtained by fitting the bias dependence of TMR ratio.

In the calculations and analysis, some intrinsic parameters can be derived or obtained by extrapolation in advance from experimental data as follows: TMR(0, T=0)=60%, the identical and effective spin-polarization of the two FM electrodes $P'=[\mathrm{TMR}(0,0)/(2+\mathrm{TMR}(0,0))]^{1/2}$=48.0%, $\rho_{\mathrm{M}}/\rho_{\mathrm{m}} = (1+P')/(1-P')$=2.846, ξ=0.6255, $1/\xi$=1.599, S=3/2, and T_{C}=900°C for the $Co_{75}Fe_{25}$ alloy, therefore $E_{\mathrm{m}} = 3k_{\mathrm{B}}T_{\mathrm{C}}/(S+1)$=121meV. The Curie temperature T_{C} and the density of states for the majority and minority itinerant electrons $\xi(\rho_{\mathrm{M}}/\rho_{\mathrm{m}})$ (i.e., spin-polarization) are the intrinsic parameters of the FM electrodes.

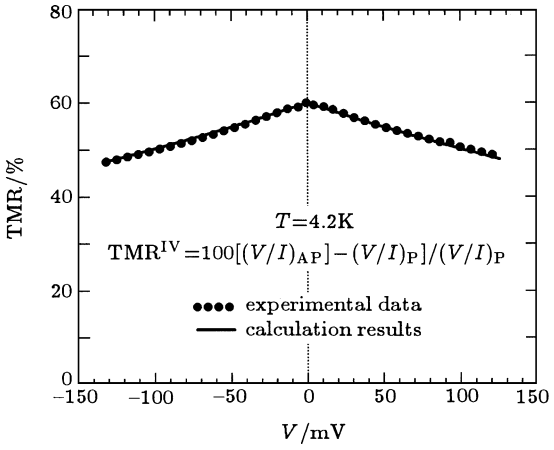


Fig.3. DC bias voltage dependence of TMR^{IV} (T=4.2K) ratio for V from 0 to ±120mV for the same annealed MTJ, as that used in Fig.1.

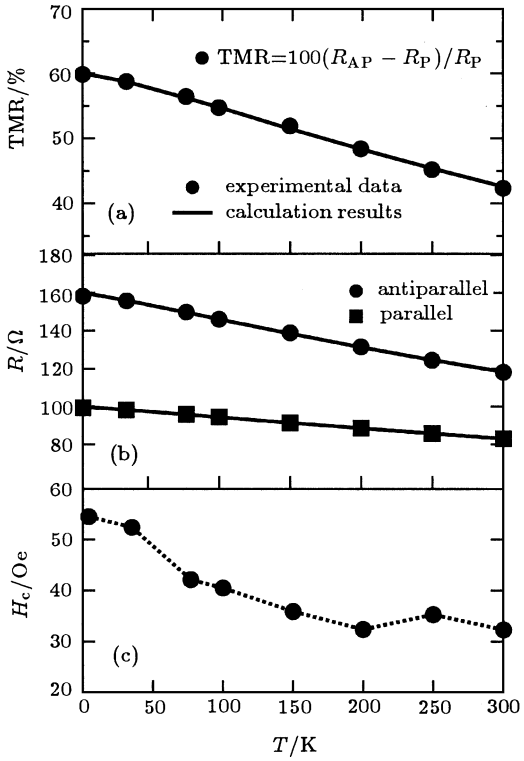


Fig.4. Temperature dependence of the TMR ratio (a), resistances (b), and coercivity (c) from 4.2 to 300 K for the MTJ.

Figure 4 shows the temperature dependence of the TMR ratio, resistance, and coercivity from 4.2 to 300K, in which each data point is deduced from TMR vs H curve at the specific temperature. Solid dots and squares are the experimental data and the solid lines represent the calculated values. The parameters E_c^{AP}=0.0061 meV and E_c^{P}=0.0032meV can be uniquely obtained by fitting the temperature dependence of resistances for the parallel (P) and antiparallel (AP) magnetization configurations, respectively, of the magnetization of the two electrodes using Eq.(7) with Q=0.0567, E_m=121mV and $V \simeq$0mV. Then, three fitting parameters of $\frac{|T^d|^2}{|T^J|^2}$, E_c^{AP}, and E_c^{P} together with other two parameters of ρ_M/ρ_m=2.846 and E_m=121mV deduced from experimental data, can be confirmed further by the calculation of the temperature dependence of TMR ratio from 4.2 to 300K at 1mV bias using Eq.(10).

Therefore, the parameters mentioned above are intrinsic and unique for a MTJ because they are only determined by the FM electrode materials and the MTJ barrier structure. They need not vary with increasing bias voltage at low bias or/and temperature from 4.2 to 300K. This means that the main magneto-electric properties of the MTJ can be self-consistently evaluated and explained using the magnon-assisted tunnelling theory and a unique set of intrinsic parameters.

Figure 5 shows the dc bias voltage dependence of TMR^{RH} ratio at T=300K, while V varies from 0 to ±500mV for the junction. Each experimental TMR^{RH} ratio was deduced from the TMR versus H curves under a finite bias between 0 and ±500mV. Opened circles are the experimental data and the solid line represents the calculated values using Eq.(10) between 0 and ±120mV, and Eq.(13) between ±121mV and ±500mV with the five intrinsic parameters of ρ_M/ρ_m = 2.846, E_m=121mV, Q=0.0567, E_c^{AP}=0.0061meV and E_c^{P}=0.0032meV obtained above.

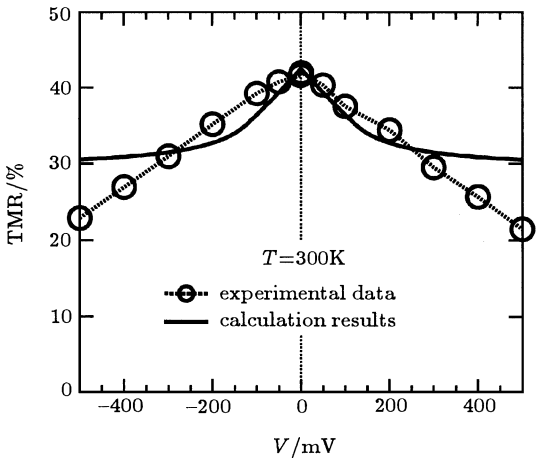


Fig.5. DC bias voltage dependence of TMR^{IV} (T=300K) ratio when V varies from 0 to ±500mV for the same annealed MTJ as that used in Fig.1.

It can be been that the dc bias voltage dependence of TMR^{IV} (V, T) ratio evaluated based on the magnon-assisted tunnelling theory at room tempera-

ture agrees well with the experimental data from 0 to ±250mV for the junction. However, the difference between the experimental and theoretical values appears at the high bias voltage of larger than 250mV. This difference comes from the fact that only two extreme cases, i.e. the completely parallel (P) and antiparallel (AP) alignments of the magnetization of the two FM electrodes, were considered in this model for evaluating the dc bias voltage or/and temperature dependence of TMR ratio and resistance (or conductance) for the junction. Other more complex alignment of the magnetization of the two electrodes, such as the vortex domain structures, was not included in this model. This is because the Zeeman interaction energy in the Hamiltonian is neglected due to its comparative smallness and complexity in calculation.[8] Therefore, in the low dc voltage biasing case the identical parallel (P) and antiparallel (AP) alignments of the magnetization of the two FM electrodes can be easily realized, and the theoretical calculation can be in good agreement with the experimental data. But in the high dc voltage biasing case (i.e. large dc current) the vortex domain structures can be formed under the dc current-induced Oersted field in the FM electrode layers, (especially in the free layer), which can lead to the deviation between the theoretical and experimental results.

In order to verify the vortex domain structures formed in the magneto-electrode at a high dc voltage (or a large dc current), micromagnetics simulations were performed using the method of minimization for energy.[20] Figure 6 shows two typical micromagnetics results of simulation for a MTJ with a size of $2.4\times2.4\mu m^2$ when a dc linear current of 11 or 13mA passes through its centre. In the simulations, the bottom magnetic electrode of $Co_{75}Fe_{25}$ (4nm) is pinned along the easy magnetic direction. However, a free layer is on the top of $Co_{75}Fe_{25}$ (4nm)/$Ni_{79}Fe_{21}$ (25nm). The total energy of the MTJ system consists of the exchange interaction energy, the magnetocrystalline anisotropy energy, the Zeeman energy under a current-induced Oersted field, and the stray field energy. The magnetocrystalline anisotropy constant, spontaneous magnetization, and exchange interaction constant of the free layer are $K_1=1.2\times10^{-3}$J/cm^3, M_S (T=300K)=0.08T, and $A=1.0\times10^{-13}$J/m respectively, and are taken from the parameters of the $Ni_{79}Fe_{21}$ alloy. The normal distribution of the magnetic grain size in the free layer is adopted. When a dc current ranging from 0.8 to 20mA passes though the centre of the MTJ, a vortex domain structure, which looks like a butterfly-shaped domain, can be gradually formed. Such a vortex domain structure can result in the decrease of net magnetization of the FM electrodes under a high voltage biasing. So the TMR ratios decrease significantly at high bias voltage (i.e. large dc current) regimes.

Figure 6 demonstrates two typical butterfly-like domain structures based on the micromagnetics simulations for the corresponding MTJ with a size of 2.4×2.4 μm^2 when a dc current of 11mA (a) or 13mA (b), passing through the centre of the MTJ.

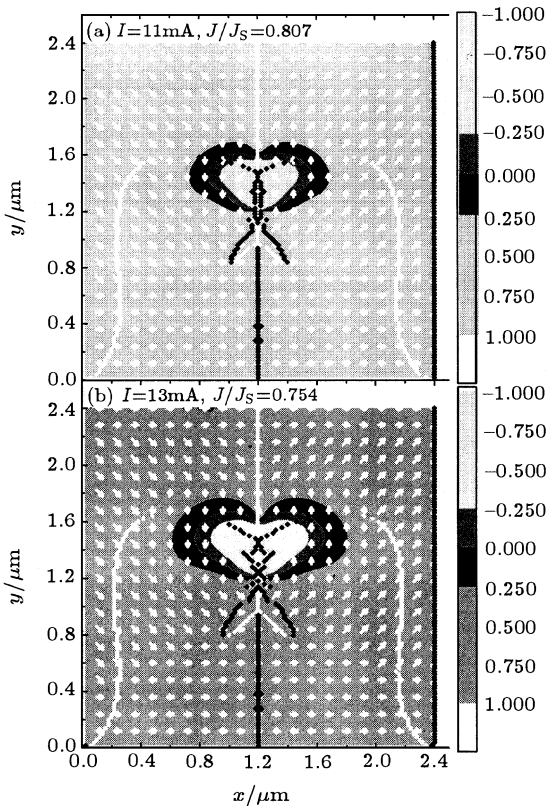


Fig.6. Two typical butterfly-like domain structures with a size of $2.4\times2.4\mu m^2$ in the magneto-electrode of the free layer for a MTJ.

A series of simulations show that the dynamic butterfly-like domains and the magnetization switching can occur in the free layer of a MTJ when a dc current in the range of 100μA to 12 mA passes through the MTJ, i.e. under a corresponding dc bias voltage of about 10 to 1000mV. Therefore, the spin-electron transport properties and the TMR ratio can be dramatically affected by the magnetization switching via the current-induced Oersted field. The butterfly-like and circular vortex domain structures formed can lead to a sharp decrease of net magnetization in the free layer.

Figure 7 shows the dc current dependence of

the normalized magnetization $J(I)/J_S(I=0)$, based on the micromagnetics simulations and the dc current dependence of the normalized TMR ratio TMR(I)/TMR(I=0) deduced from the experimental data for the MTJ at room temperature. The normalized magnetization of the free layer decreases with increasing dc current I, showing a similar decay manner to the TMR(I)/TMR(I=0).

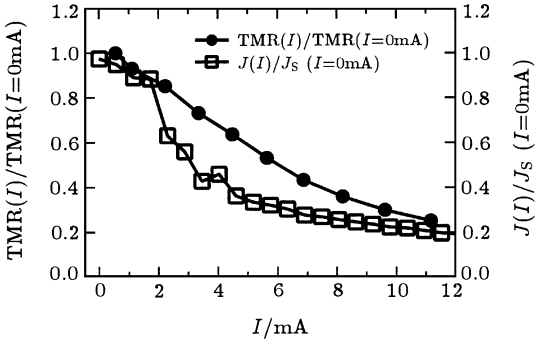


Fig.7. DC current I dependences of the normalized magnetization $J(I)/J_S(I = 0)$ and TMR ratio TMR(I)/TMR(I=0) for a MTJ at room temperature.

5. Conclusion

In conclusion, a dc current-induced Oersted field could lead to the formation of butterfly-like-vortex domain structures and local magnetization reversals in the FM electrodes—especially in the free layer of the MTJs. The micromagnetics simulation shows that the butterfly-like vortex domain structures can decrease the net magnetization values of the FM electrodes under a high voltage biasing, and so the TMR ratios decrease significantly in high bias voltage (i.e. large dc current) regimes. Therefore, Zeeman interaction energy should be considered in a perfect theory for analyzing the magneto-electronic properties of the MTJs when large biasing voltages are applied across the junctions. It is not only in order to improve the self-consistent calculation of magnetoelectric properties for a MTJ, but also in order to evaluate the magnetization curves (i.e. loops) of the same MTJ that we use the magnon-assisted tunnelling theory with a unique set of intrinsic parameters in the study.

References

[1] Daughton J M 1997 *J. Appl. Phys.* **81** 3758

[2] Tehrani S, Chen E, Durlam M, DeHerrera M, Slaughter J M, Shi J and Kerszykowski G 1999 *J. Appl. Phys.* **85** 5822

[3] Parkin S S P, Roche K P, Samant M G, Rice P M, Beyers R B, Scheuerlein R E, O'Sullivan E J, Brown S L, Bucchigano J, Abraham D W, Lu Y, Rooks M, Trouilloud P L, Wanner R A and Gallagher W J 1999 *J. Appl. Phys.* **85** 5828

[4] Han X F, Oogane M, Kubota H, Ando Y and Miyazaki T 2000 *Appl. Phys. Lett.* **77** 283

[5] Freitas P P, Cardoso S, Sousa R, Ku W J, Ferreira R, Chu V and Conde J P 2000 *IEEE Trans. Magn.* **36** 2796

[6] Stein S, Schmitz R and Kohlstedt H 2001 *Solid State Commun.* **117** 599

[7] Machida K, Hayashi N, Miyamoto Y, Tamaki T and Okuda H 2000 *J. Magn. Magn. Mater.* **235** 201

[8] Zhang S, Levy P M, Marley A C and Parkin S S P 1997 *Phys. Rev. Lett.* **79** 3744

[9] Bratkovsky A M 1998 *Appl. Phys. Lett.* **72** 2334

[10] Han X F, Murai J, Ando Y, Kubota H and Miyazaki T 2001 *Appl. Phys. Lett.* **78** 2533

[11] Han X F, Yu A C C, Oogane M, Murai J, Daibou T and Miyazaki T 2001 *Phys. Rev.* B **63** 224404

[12] Egeloff W F, Chen P J, McMichael R D, Powell C J, Deslattes R D, Serpa F G and Gomez R D 2001 *J. Appl. Phys.* **89** 5209

[13] Yuasa S, Nagahama T and Suzuki Y 2002 *Science* **297** 234

[14] LeClair P, Kohlhepp J T, van de Vin C H, Wieldraaijer H, Swagten H J M, de Jonge J M, Davis A H, MacLaren J M, Moodera J S and Jansen R 2002 *Phys. Rev. Lett.* **88** 107201

[15] Peng Z L, Wang W N, Zhu T, Han X F and Zhan W S 2003 *Acta Phys. Sin.* **52** 2901 (in Chinese)

[16] You C, Zhao Y P, Jin E J, Li F F, Wang T X, Zeng Z M and Peng Z L 2004 *Acta Phys. Sin.* **53** 2741 (in Chinese)

[17] Jullière M 1975 *Phys. Lett.* **54**A 225

[18] Simmons J G 1963 *J. Appl. Phys.* **34** 1793

[19] Brinkman W F, Dynes R C and Rowell J M 1970 *J. Appl. Phys.* **41** 1915

[20] Zhao S F, Jin H M, Wang X F and Yan Y 2001 *J. Phys.: Condens. Matter* **13** 3865